

Article

Electrospun Polyurethane Vascular Grafts for Cerebral Revascularization: A Pilot Study on Rats

Evelynn Vergauwen ^{1,*}, Michiel R. L. Tubeeckx ^{2,†}, Annemie Houben ³, Sandra Van Vlierberghe ³, Marc Demolder ⁴, Guido R. Y. De Meyer ⁴, Patrick Pauwels ⁵ and Tomas Menovsky ⁶

¹ Department of Neurology, University of Antwerp, Universiteitsplein 1, 2610 Antwerpen, Belgium

² Department of Internal Medicine, University of Antwerp, 2610 Antwerp, Belgium; michiel.tubeeckx@gmail.com

³ Department of Organic and Macromolecular Chemistry, Centre of Macromolecular Chemistry, Ghent University, 9000 Ghent, Belgium

⁴ Department of Physiopharmacology, University of Antwerp, 2610 Antwerp, Belgium

⁵ Department of Anatomopathology, University Hospital Antwerp, University of Antwerp, 2610 Antwerp, Belgium

⁶ Department of Neurosurgery, University Hospital Antwerp, University of Antwerp, 2610 Antwerp, Belgium

* Correspondence: evelynn-v@hotmail.com

† These authors contributed equally to this work.

Abstract: The current standard technique for vascular grafting in cerebral revascularization surgery employs the interposition of an autologous blood vessel. Technical complications have necessitated the development of a synthetic alternative, but classical biomaterials are not suited for small caliber vascular grafting due to the resulting neointimal hyperplasia and thrombosis. The electrospinning of polymers is a promising technique for the development of small vascular grafts. The in vivo performance and efficacy of electrospun polyurethane (ePU) grafts with an internal diameter of <1.5 mm have thus far not been evaluated. We developed a novel ePU graft, with a diameter of 1.25 mm, for implantation into the infrarenal aorta of rats. The patency rates of grafts after a 4-month period were equal to those reported in other studies using larger ePU graft diameters and equal or higher than in studies employing other biomaterials. We observed some loss in flow velocity throughout the grafts, which suggests a decreased elasticity of the graft compared to that of the native rat aorta. However, the grafts demonstrated good neo-endothelialization and minimal neointimal hyperplasia. Their porosity promoted cellular infiltration, as observed under tissue slide examination. Our results show that ePU vascular grafts with an internal diameter of <1.5 mm are promising candidates for vascular grafting in cerebral revascularization surgery.

Keywords: cerebral bypass; cerebral revascularization; electrospun polyurethane; vascular graft; vascular neurosurgery



Citation: Vergauwen, E.; Tubeeckx, M.R.L.; Houben, A.; Van Vlierberghe, S.; Demolder, M.; De Meyer, G.R.Y.; Pauwels, P.; Menovsky, T. Electrospun Polyurethane Vascular Grafts for Cerebral Revascularization: A Pilot Study on Rats. *BioChem* **2024**, *4*, 1–17. <https://doi.org/10.3390/biochem4010001>

Academic Editor:
Nidhi Jalan-Sakrikar

Received: 3 November 2023

Revised: 9 December 2023

Accepted: 15 December 2023

Published: 5 January 2024



Copyright: © 2024 by the authors. Licensee MDPI, Basel, Switzerland. This article is an open access article distributed under the terms and conditions of the Creative Commons Attribution (CC BY) license (<https://creativecommons.org/licenses/by/4.0/>).

1. Introduction

Cerebral revascularization is a microsurgical procedure that is used for the augmentation or preservation of blood flow to certain brain regions. Revascularization of brain tissue can be performed either through a bypass from the extracranial circulation to the intracranial circulation (EC-IC bypass) or through the interconnection of two intracranial vessels (IC-IC bypass). One example of the augmentation of blood flow is a bypass between the superficial temporal artery and the medial cerebral artery (STA-MCA) in patients with internal carotid artery (ICA) stenosis. On the other hand, the preservation of blood flow consists of the maintenance of an existing vascular conduit, for instance, after removal of a complex brain aneurysm or a skull base tumor with vascular invasion [1].

Often, a tension free anastomosis cannot be obtained without the interposition of a vascular graft, usually the great saphenous vein (GSV) (inner diameter (ID): 4.9 ± 0.9 mm)

or the radial artery (RA) (ID: 3.55 ± 0.45 mm) [2,3]. The choice of a vascular graft depends on the required flow delivery, the size of the recipient vessel, and the availability of the donor vessel [4]. The advantages of the GSV include its length and the absence of atherosclerosis or vasospasm. The disadvantages of GSV include its large ID, its lower long-term patency rates (overall 80%) compared to those of RA grafts (overall 90%), as well as thrombogenic valves and varicose veins [5,6]. The advantages of the RA include its anatomical similarity to cerebral arteries, the facilitation of surgical anastomosis, and its allowance for greater fluctuations in arterial blood pressure. The disadvantages include its short length and the potential vascular compromising of the hand [7]. Additionally, the harvesting of both autologous grafts can be time-consuming and invasive for the patient. Thus, there is a medical need for an effective synthetic alternative for cerebral revascularization. The advantages of a synthetic alternative graft could include a reduction in vasospasm, vasculopathy, flow-mismatch, wound infection of the donor site, and the prevention of vascular compromise or availability issues.

As the IDs of cerebral vessels typically range from 1.07 ± 0.29 mm (cortical segment of anterior inferior cerebellar artery, AICA) to 8.57 ± 1.34 mm (cervical portion of the ICA), synthetic grafts with IDs < 6 mm could offer the greatest therapeutic advantages [8]. To date, there is little or no data indicating the effectiveness of small caliber (ID < 6 mm) synthetic cerebral vascular grafts. Nevertheless, great progress has been made in the search for synthetic grafts in cardiovascular surgery. However, the use of classical biomaterials, such as polytetrafluoroethylene (PTFE) and polyethylene terephthalate (PET), has been limited to large caliber (ID ≥ 6 mm) cardiovascular surgery [9,10]. Some animal studies using PTFE and PET grafts with ID < 6 mm have reported discouraging patency rates (overall 40% at six months) due to dynamic non-compliance, surface thrombosis, and neointimal hyperplasia (NIH), which become more critical with the gradual reduction of the graft ID [11–14].

An attempt to increase patency rates in small caliber cardiovascular grafting was recently made by the use of electrospinning, a technique that produces nanoscale fibers through the acceleration of a charged polymer fluid towards a rotating collector [15]. From a morphological point of view, the porosity, high surface-to-volume ratio, and surface topography of electrospun grafts mimic the extracellular matrix of native blood vessels. This resemblance promotes tissue reorganization through nutrient transfer, gas exchange, and intercellular communication. In various *in vitro* and *in vivo* settings, these processes have been shown to counteract thrombosis and NIH and improve neo-endothelialization (NE) [10,16].

Many *in vitro* and *in vivo* animal electrospinning studies, using various electrospun polymeric biomaterials, have demonstrated the superior efficacy of electrospun polyurethane (ePU). ePU demonstrates anti-thrombogenic properties, biocompatibility, and a mechanical strength and elasticity that closely matches the native vessel capacities [12,17,18]. Therefore, ePU grafts are promising substitutes for small caliber vascular replacement, and indeed, they are already used to achieve vascular access in hemodialysis patients (ID 6 mm) [10]. However, the efficacy of ePU grafts with an ID < 1.5 mm has not been determined to date. To address the important question of whether ePU grafts with an ID < 1.5 mm are clinically effective, we developed a novel ePU graft with an ID of 1.25 mm, and we determined its efficacy after implantation into the infrarenal aorta of rats in a small pilot study. For this study, the infrarenal aorta was used, as it has comparable dimensions and hemodynamics to those of human cerebral vessels, hence rendering our findings clinically relevant [19].

2. Methods

In a preclinical pilot animal study, in-house generated ePU grafts were implanted into the infrarenal aorta of rats. After a period of four months, our novel ePU graft was assessed for patency, thrombosis, NIH, and NE. The patency and thrombosis results were compared to those of the control group comprised of rats that underwent sham surgery. As NIH is

not a natural feature of native rat aorta, and endothelial coverage is typically 100%, the results of NIH and NE in regards to histology were only quantitatively described in the intervention group. The research hypothesis was that the intervention group (ePU graft implantations) would exhibit non-inferiority towards a control group (those undergoing sham surgeries) regarding the incidence of aortic patency and thrombosis. Second, we expected minimal differences in hemodynamic performance between the groups. Third, we expected minimal NIH, as well as confluent coverage of the luminal surface with NE throughout the proximal, mid-portion, and distal graft.

2.1. Graft Production: Polyurethane Solution and Electrospinning

Electrospinning of the graft was performed using a novel device designed by the technical workshop (CWFV) of Ghent University—Faculty of Sciences, consisting of three main components: (1) a power supply (Glassman High Voltage, EL50P00, High Bridge, NJ, USA) capable of generating a potential between 0 and 50 kV; (2) a 6 syringe motor driven pumping system (New Era Pump System, Multi-phaser NE1600, Farmingdale, NY, USA); and (3) a grounded mandrel in a rotating unit for the collection of the fiber jet (Figure 1). A liquid 5% (m/m) solution was prepared by dissolving non-biodegradable polyurethane pellets (Carbothane[®], Aliphatic TPU Clear Series, PC3575A, Velox Lubrizol, Hamburg, Germany) in chloroform (Chem-lab, Zedelgem, Belgium) at room temperature (15–25 °C). A 20 mL syringe was filled with the solution and positioned in the automatic dispenser unit. The flow (flow rate: 1 mL/h) was passed through a distally mounted tube with a blunt end 22-gauge needle. The needle tip was positioned vertically at a distance of 8 cm from a 1.0 mm diameter zinc mandrel. The mandrel had been coated with molten (80 °C) polyethylene glycol (PEG, Fluka-Sigma Aldrich, Buchs, Switzerland) and dried for 24 h at room temperature (15–25 °C). The PEG-coated zinc mandrel was mounted on a rotating unit (speed: 275 rotations per minute). After completion of this setup, the voltage source was set at 20 V (direct current), and consequently, the charged polyurethane solution was accelerated from the anode (needle tip) to the cathode (rotating mandrel/background electrode). Electrospinning was performed for one hour. The mandrel, circumferentially covered with a fine ePU mesh (the graft), was subsequently placed in distilled water for 1 h to dissolve the PEG coating, facilitating the detachment of the graft. The collected grafts were dried for two hours at 40 °C in atmospheric pressure to evaporate the residual chloroform. The ePU grafts were sterilized in a 100% ethylene oxide cold cycle process of 38 °C (Sint-Jan Hospital, Bruges, Belgium).

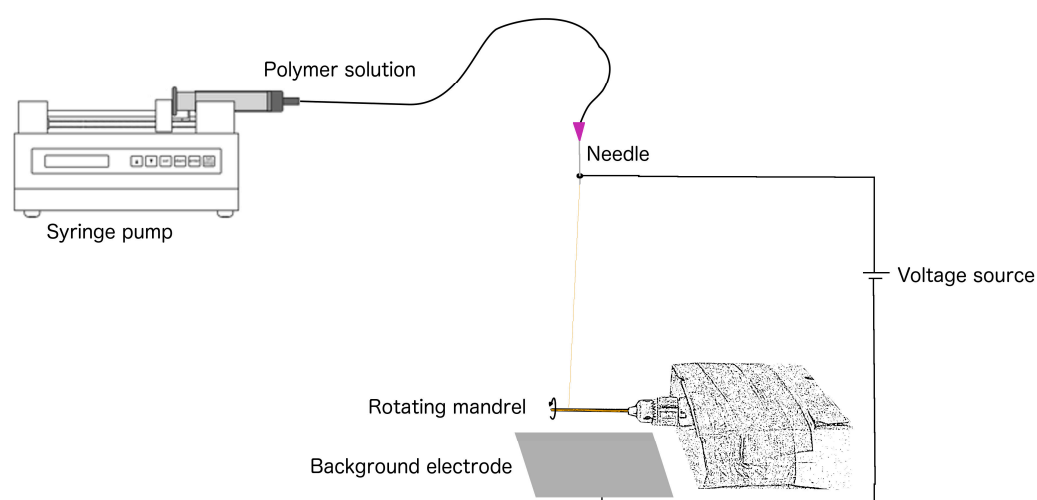


Figure 1. Electrospinning. The polyurethane solution was pumped through a tube, distally ending in a needle. At the needle tip, the surface tension of the droplets was overcome by the power of the voltage source. The droplets were accelerated as fibers and collected onto the rotating mandrel, which was attracted by the background electrode.

2.2. SEM: ePU Graft Characterization

Before sterilization, a 1 mm piece was cut from one of the ePU grafts and sputter-coated with gold. The specimen was visualized with scanning electron microscopy (SEM) (Fei, Quanta Field Emission Gun 200, Hillsboro, OR, USA), and the images were analyzed using ZEN 2 core software for size calibration (Carl Zeiss AG, Oberkochen, Germany). The gross morphology, surface topography, fiber diameter, pore size, and wall thickness were assessed on 24 randomly selected regions and expressed as the mean \pm SD (in μm).

2.3. Animal Characterization and Grouping

For these experiments, 18 male Wistar Han International Genetic Standard (IGS) rats (*Rattus norvegicus*, Charles River, France) were used, and this study was approved by the Ethical Committee for Animal Experiments at the University of Antwerp (approval number 2015-55). The rats were 9 weeks of age (weighing 276–300 g) at the start of the study and were all preoperatively healthy. All experiments were conducted according to the Guide for the Care and Use of Laboratory Animals of the National Institutes of Health [20], and the experiments were reported according to the ARRIVE guidelines [21]. All the rats were housed pairwise in the animal unit of the University of Antwerp. At the start of the study, the rats were randomly divided (using computer assistance) into two groups: the intervention group ($n = 9$, ePU graft surgery) and the control group ($N = 9$, sham surgery).

2.4. Implantation of ePU Grafts

In the intervention group, an ePU graft (ID: 1.25 mm, length: 7.50 mm) was implanted into the infrarenal aorta using a surgical microscope (Carton SPZ50, Tokyo, Japan). A midline laparotomy was performed, extending from the xiphoid to just above the bladder, and the intestines were laid aside, exposing the retroperitoneal space. After dissection, two temporary aneurysm clamps (Peter Lazic, Tuttlingen, Germany) were placed on the infrarenal aorta, above the iliac bifurcation. The aorta was completely transected halfway between the clamps. The last millimeters of each stump were stripped from the adventitial layer and flushed with sterile saline. The graft was implanted using two end-to-end anastomoses with circumferentially interrupted non-absorbable 10-0 sutures (Ethilon, Somerville, NJ, USA). Before the last suture, the graft lumen was flushed with sterile saline. In the control group the infrarenal aorta was clamped, divided over the superior portion of its circumference, and reanastomosed using the same interrupted sutures. All surgeries were performed under general inhalation anesthesia using isoflurane (5% induction and 2–3% maintenance concentrations, Forene[®] Abbott, Chicago, IL, USA) in an O₂ enriched gas mixture. Body temperature was rectally monitored and corrected with an underlying heating pad. Vital signs were monitored using MouseOx software (Starr Life Sciences, Oakmont, PA, USA). No anticoagulant or antiplatelet drugs were used. Subcutaneous buprenorphine (0.1 mg/mL) (Vetergesic[®] Ecuphar, Oostkamp, Belgium) was administered as an analgesic premedication. Postoperatively, the following products were administered: epicutaneous chlorhexidine chloride (Astrexine[®] Pierre Fabre, Anderlecht, Belgium), epicutaneous lidocaine hydrochloride 2% (Xylocaine[®] AstraZeneca, Ukkel, Belgium), subcutaneous buprenorphine 0.1 mg/mL (Vetergesic[®] Ecuphar, Oostkamp, Belgium), and subcutaneous amoxicillin 150 mg/mL (Duphamox LA[®] Zoetis, Zaventem, Belgium).

2.5. In Vivo Assessments over a 4-Month Period: Thrombosis

Aortic thrombosis in the intervention and control group was clinically assessed over a 4-month period. The following parameters were used for the evaluation of thrombosis of the lower limb: skin/paw pad temperature (cold) and color (cyanosis/pallor), ulceration, paresis/paralysis, and limb pain (biting or shaking limb). Intestinal thrombosis was evaluated by the assessment of abdominal tenderness during handling, a loss of appetite, and alterations in fecal matter and production (blood, constipation) [22].

2.6. *In Vivo Assessments after a 4-Month Period: Patency*

In vivo evaluation of patency in the intervention and control group was performed after a 4-month period using an ultrasound system (Visualsonics, Vevo[®] 2100, Amsterdam, The Netherlands). This system operated at a high frequency (13–75 MHz), with a spatial resolution of ~30 microns and a temporal resolution of 1000 frames/sec. Ultrasound imaging on the rats was performed under general anesthesia using sevoflurane (5% induction and 2% maintenance, Sevoflurane[®] Abbvie, Wavre, Belgium) in an O₂ enriched gas mixture. The abdomen was shaved, and 37 °C ultrasound gel was applied. The probe was levelled perpendicular to the spine. Using a pulsed-wave 40 MHz Doppler in the coronal plane, patency was categorically evaluated by the presence (patent) or absence (non-patent) of pulsatile arterial flow in the aorta segment distal to the graft/control aorta. Absolute maximal flow velocity (Vmax) and Vmax decay from the proximal to distal graft/control aorta were measured in the sagittal plane and expressed as the mean ± SD (in mm/s). The inner/outer and proximal/distal diameters and the systolic/diastolic diameters of the graft/control aortas (IDps, IDpd, IDds, IDdd, ODps, ODpd, Odds, and ODpd) were measured using the motion-mode (in µm) and compared between the groups. The images were analyzed using ImageJ software (ImageJ, National Institutes of Health). The systolic expansion was calculated using the formula [IDps – IDpd] for the proximal segment and [IDds – IDdd] for the distal segment. The proximal to distal decay in the graft/control aorta expansion [(IDps-IDpd) – (IDds-IDdd)] was calculated and compared between groups.

2.7. *Retrieval Surgery after 4-Month Period*

After ultrasound imaging, retrieval surgery of the ePU grafts/control aortas was performed. The same procedure, medication, and anesthetic products as those described for the implantation were used (see above). In between two temporary clamps, either the graft (intervention group) or a 7.5 mm piece of reanastomosed control aorta (control group) was retrieved. All rats were subsequently sacrificed with an intracardiac injection of 1.5 mL sodium pentobarbital 60 mg/mL (Nembutal[®] Ceva, Libourne, France).

2.8. *Histological Assessments of Retrieved ePU Grafts: NIH and NE*

The retrieved ePU grafts were embedded in 4% formaldehyde for 24 h and were subsequently placed in 60% isopropyl alcohol. After dehydration and tissue preparation using an automated device (Excelsior, Thermo Fisher Scientific, Breda, The Netherlands), the samples were fixed using an automated paraffin embedding device (TES 99, Medite, Burgdorf, Germany). Two longitudinal sections of 5 µm thickness were cut from the samples. A standard light microscope (Olympus BX41) with imaging software (Leica Application Suite X, Leica, Wetzlar, Germany) was used for visualization. One slide from each rat was stained with hematoxylin and eosin (H&E), for the evaluation of NIH in the ePU grafts. NIH was quantified as the thickness (in µm) of the area between the endothelial layer and luminal graft surface. It was measured in three different regions: (1) the first anastomosis, (2) mid-graft, and (3) the second anastomosis. For each region, two measurements were circumferentially performed, 180 degrees apart from each other. NIH was expressed as the mean ± SD for each region. The length of NIH (in mm) was the sum of all longitudinal NIH regions, measured as close as possible to the endothelial layer, in a longitudinal manner between both ends of the graft, superiorly and inferiorly (Figure 2). The length was compared to the total length (in mm) of the ePU graft and expressed as a percentage (length/length %). The second slide was stained with anti-Factor VIII (anti-von Willebrand Factor, Dako, Glostrup, Denmark) antibody for the identification of endothelial cells. NE was quantified as anti-F VIII positive length (in mm), compared to the total length (in mm) of the ePU graft and expressed as a percentage (length/length %).



Figure 2. Measurement of NIH on histological slides. Graphical representation of a graft. NIH = sum of the grey parts in the superior and inferior lumen.

2.9. Statistical Analyses

Statistical analyses were conducted using SPSS software (Statistical Package for the Social Science version 24, IBM analytics). No statistical analyses were performed to compare the incidence of aortic patency and thrombosis in the intervention group to that of the control group, and these parameters were only quantitatively described. Ultrasound data on hemodynamic performance were analyzed using a one-way ANOVA and Student's *t*-test to compare the mean values among single groups and between the two groups, respectively. The histological data of NIH were analyzed using a one-way ANOVA test to compare the mean values in the intervention group. NIH and NE were quantitatively described. The assumptions of the tests were confirmed by the data. The significance level was set at $p < 0.05$.

3. Results

3.1. Pre-Implant Characterization: SEM

The features of one ePU graft were analyzed using SEM imaging. In Figure 3, the tubular gross morphology and porous surface topography of the ePU graft are presented. The fibers were randomly oriented, and small irregularly distributed beads were observed on the course of some fibers. The mean fiber diameter of the ePU graft was $2.02 \pm 1.43 \mu\text{m}$ (minimum $0.30 \mu\text{m}$, maximum $5.17 \mu\text{m}$). The graft exhibited a mean pore size of $5.65 \pm 2.30 \mu\text{m}$ (minimum $2.33 \mu\text{m}$, maximum $11.66 \mu\text{m}$) and a wall thickness of $223 \pm 18 \mu\text{m}$ (minimum $189 \mu\text{m}$, maximum $260 \mu\text{m}$). The presence of PEG-residue was not evaluated because the sample size was too small.

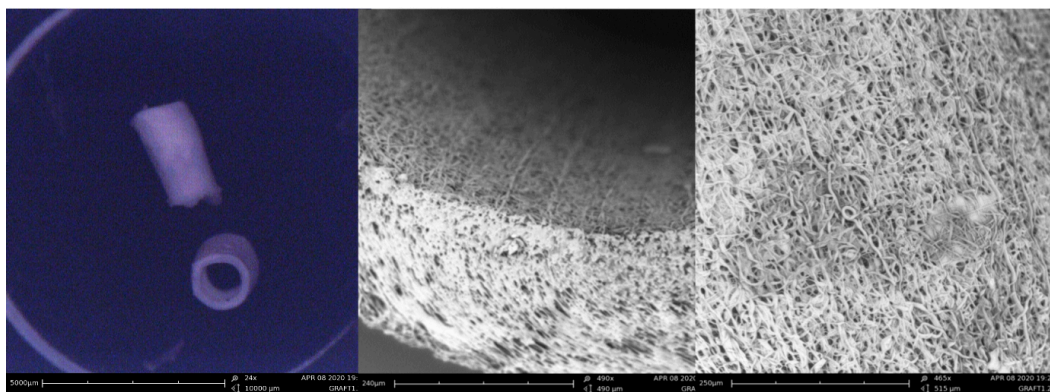


Figure 3. SEM images. Left (24 \times): the gross morphology demonstrates a regularly shaped tubular graft with an ID of 1.25 mm. Middle (490 \times): smooth inner luminal curvature, with occasional small irregularly distributed beads on the course of some fibers. Right (465 \times): surface topography showing a nanofiber porous mesh of electrospun polyurethane.

3.2. Implantation of ePU Grafts

All rats were preoperatively healthy, as evaluated using standardized welfare control sheets. Throughout the experiments, a total of four rats from the intervention group were excluded from the study. In two of them, surgery was prematurely terminated without interposition of a graft, due to (1) technical problems with the microscope and (2) the inability to reach sufficient levels of anesthesia. The other two rats died because of (3) major intraoperative bleeding due to accidental injury of the vena cava and (4) anesthetic intolerance. These four subjects were replaced by four unused Wistar Han IGS rats from the same lot. In the intervention and control group, all graft/control aorta anastomoses were

tension-free, and no major complications occurred. When releasing the vessel clamps after the procedure, an optical check of all graft/control aortas showed good expansile pulsations. The grafts became red and saturated with blood, indicating permeability to the erythrocytes, but without any leakage at the anastomoses (Figure 4). Small anastomotic leakage was terminated using a hemostatic patch (Surgicel[®], Ethicon, Johnson&Johnson, Sommerville, NJ, USA). The immediate postoperative outcome for all rats was clinically favorable.

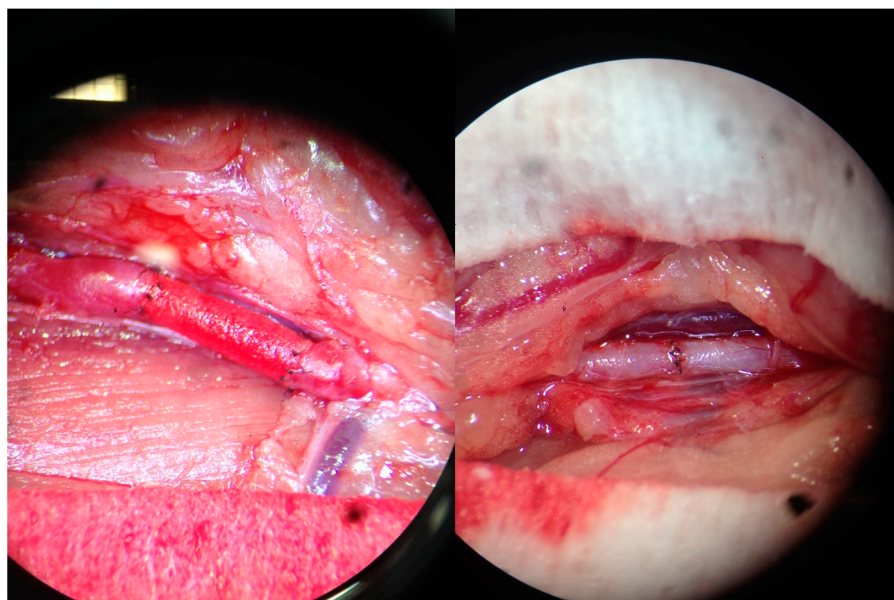


Figure 4. Implantation surgery. (Left): intervention group, end-to-end anastomosis of a 1.25 mm ID ePU graft to the infrarenal aorta. (Right): control group, end-to-end anastomosis of partially transected infrarenal aorta. Images captured by a camera through the microscope lens.

3.3. *In Vivo* Assessments: Clinical Parameters of Thrombosis

On the first postoperative day, one rat out of nine in the intervention group developed a paraparesis of the lower limbs, suggesting graft thrombosis. Humane endpoints were met, and the rat was euthanized. Postmortem *ex vivo* examination of the graft could not determine the cause of thrombosis. However, subsequent histological evaluations with H&E staining demonstrated a large thrombus, occluding the graft lumen. Thrombosis was likely caused by a surgical complication (see: Section 4). During the 4-month study-period, no other clinical parameters of aortic thrombosis were observed, either in the intervention or in the control group. The paraplegic rat was considered to exhibit graft thrombosis, bringing the overall thrombosis incidence of the intervention group to 1/9 (11%) compared to 0/9 (0%) in the control group. From a clinical surgical point of view, as further described in Section 4, we found this difference in thrombosis incidence between the intervention and the control group to be insignificant.

3.4. *In Vivo* Assessments: Patency on Ultrasound

After a 4-month period, a pulsed-wave Doppler ultrasound was used to evaluate the patency of the ePU graft/control aortas. A pulsatile arterial flow was noted in all aorta segments located distally from the graft/control aortas. No stenotic processes were detected over the course of the graft/control aortas, and there was no evidence of ePU graft-related complications, such as graft rupture or aneurysm formation. The rat with paraparesis was clinically determined to show graft failure/non-patent, bringing the overall patency of the intervention group to 8/9 (89%) compared to 9/9 (100%) in the control group. From a clinical surgical point of view, we considered this as a nonsignificant difference in patency between the intervention and the control groups. The ultrasound imaging of the ePU grafts is shown in Figure 5.

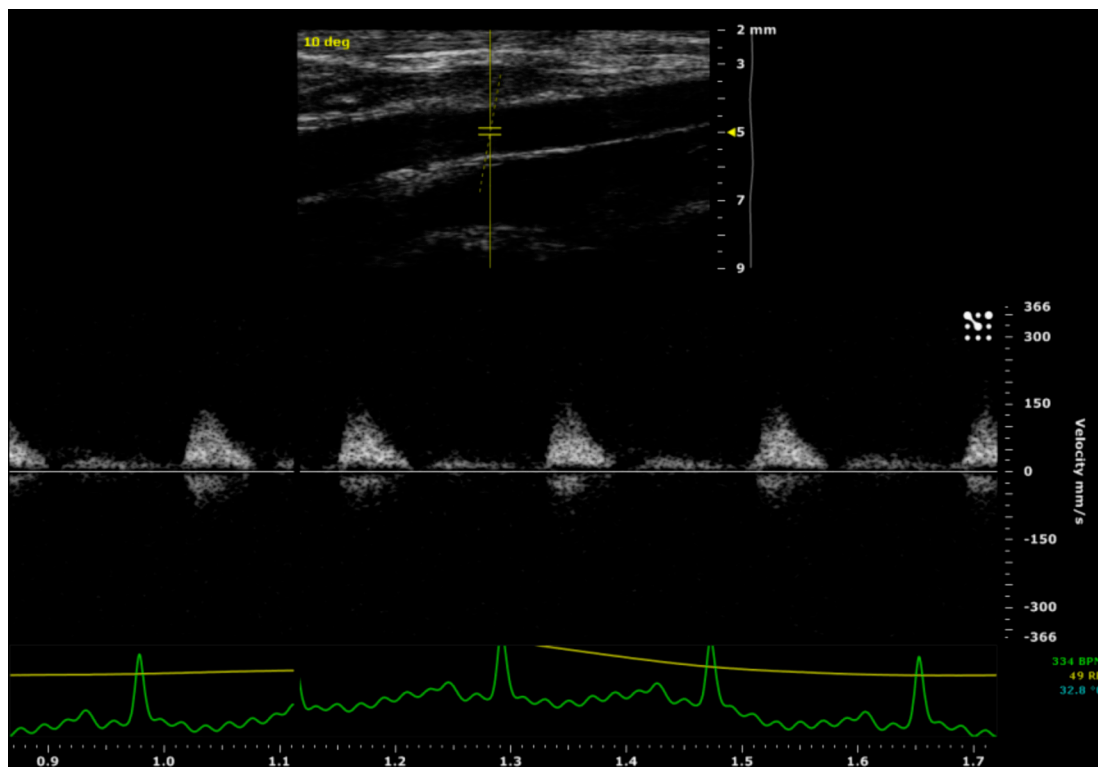


Figure 5. Ultrasound imaging of an ePU graft. Velocity of aortic blood flow was measured using pulsed-wave Doppler (left), and aortic pulsatile expansion was measured using motion-mode (right).

There was no statistically significant difference between the intervention and control group for the absolute Vmax in the proximal aorta ($p = 0.479$) and the absolute Vmax in the distal aorta ($p = 0.711$). However, there was a statistically significant difference ($p = 0.010$) in Vmax decay (from proximal to distal) between the intervention group (mean = 49 ± 40 mm/s) and the control group (mean = -14 ± 39 mm/s). These data are shown in Table 1.

Table 1. Aortic diameter and diastolic–systolic expansion with motion-mode, aortic Vmax with pulsed-wave Doppler, and the intervention and control group. The aortic systolic expansion, the aortic diastolic expansion, and the aortic expansion decay (proximal minus distal) were not significantly different between groups. There was a statistically significant difference in Vmax decay between the intervention group (49 ± 40 mm/s) and the control group (-14 ± 39 mm/s). Vmax in the mid graft was lower compared to that of the proximal and distal aorta.

		Intervention Group (N = 9)	Control Group (N = 9)	Significance of Difference (p-Value)
Proximal graft	Diastole	ID	1597 ± 365	0.083
		OD	1956 ± 402	0.083
	Systole	ID	1754 ± 370	0.054
		OD	2077 ± 399	0.066
Expansion (IDs-IDd)		157 ± 75	123 ± 49	0.280
Vmax (mm/s)		371 ± 505	250 ± 55	0.479
Mid graft	Diastole	ID	1378 ± 130	/
		OD	1766 ± 149	/
	Systole	ID	1498 ± 150	/
		OD	1826 ± 131	/
Expansion (IDs-IDd)		121 ± 55	/	/
Vmax (mm/s)		207 ± 110	/	/

Table 1. Cont.

		Intervention Group (N = 9)	Control Group (N = 9)	Significance of Difference (<i>p</i> -Value)
Distal graft Diastole	ID	1341 ± 201	1210 ± 227	0.231
	OD	1716 ± 201	1523 ± 214	0.075
Systole	ID	1445 ± 192	1324 ± 238	0.270
	OD	1803 ± 188	1620 ± 211	0.079
Expansion (IDs-IDd)		104 ± 64	114 ± 102	0.827
Vmax (mm/s)		323 ± 469	264 ± 42	0.711
Prox-dist expansion		52 ± 110	9 ± 75	0.353
Vmax decay (prox-dist, mms/s)		49 ± 40	-14 ± 39	0.010

Notes: All data are shown as means (SD) (μm), unless indicated otherwise. Vmax: maximal flow velocity; ID: inner diameter; OD: outer diameter.

There was no statistically significant difference ($p = 0.280$) in proximal aortic systolic expansion between the grafts (mean = $123 \pm 49 \mu\text{m}$) and the shams (mean = $157 \pm 75 \mu\text{m}$). Neither was there a significant difference ($p = 0.827$) in distal aortic systolic expansion between the intervention group (mean = $104 \pm 64 \mu\text{m}$) and the control group (mean = $114 \pm 102 \mu\text{m}$). There was also no statistically significant ($p = 0.353$) difference between the intervention and control group in regards to the aortic expansion decay between the proximal and distal aorta [(IDps-IDpd) – (IDds-IDdd)]. However, the means showed a relevant difference between the intervention group (mean = $52 \pm 110 \mu\text{m}$) and the control group (mean = $9 \pm 75 \mu\text{m}$). These data are summarized in Table 1.

3.5. Retrieval Surgery after a 4-Month Period

Immediately after ultrasound imaging, surgery to retrieve the ePU grafts/control aortas was performed. In vivo evaluation demonstrated good healing of the anastomoses and good expansile pulsations in the grafts/control aortas. There were no stenotic adhesions to the surrounding retroperitoneal tissue.

3.6. Histological Assessment: NIH and NE

After a 4-month period, histological analyses were performed for the evaluation of NIH and NE in the intervention group. As expected, on the first postoperative day, it was too soon to identify NIH or NE on the slides from the euthanized rat with paraparesis. Histological evaluation in this rat using H&E staining demonstrated a large thrombus, occluding the graft lumen. Therefore, only 8 out of 9 subjects were included in the histological analyses. The porous fiber mesh of the ePU graft was clearly visualized using H&E staining, and it was apparent that there was an ingrowth of different cells in the graft. NIH in the intervention group was measured on the H&E stained slides of the ePU grafts. The mean neointimal thickness of the mid graft ($35 \pm 40 \mu\text{m}$) was similar ($p = 0.978$) to that near the anastomoses ($35 \pm 43 \mu\text{m}$). In 1 of 8 ePU grafts, no NIH could be observed ($0 \mu\text{m}$). The mean percentage of the longitudinal length of the graft covered with NIH was $54 \pm 29\%$ (minimum 0%, maximum 94%). The absolute mean length of the graft covered with NIH was $6.02 \pm 4.16 \text{ mm}$ for a mean total graft length of $11.19 \pm 2.48 \text{ mm}$. These data are summarized in Table 2. An example of NIH is shown in Figure 6.

Table 2. NIH on H&E staining in the intervention group. The mean NIH was approximately equal in all regions ($\pm 35 \mu\text{m}$) and covered $\pm 54\%$ of the graft length. A total of 1/8 of the grafts showed no NIH.

Subject	Graft Length ^a (mm)	NIH Length (mm)	Graft Length/NIH Length (%)	NIH 1 ^b Anastomosis (μm)	NIH 2 ^b Anastomosis (μm)	NIH 3 ^b Anastomosis (μm)	NIH 4 ^b Anastomosis (μm)	NIH 5 ^c Mid Graft (μm)	NIH 6 ^c Mid Graft (μm)
1	9.20	6.03	66%	62	93	0	0	82	0
2	10.63	5.81	55%	50	0	77	39	82	40
3	14.38	0.00	0%	0	0	0	0	0	0
4	9.88	3.42	35%	0	0	33	55	0	27
5	16.09	14.10	88%	100	200	64	0	137	68
6	9.15	5.36	59%	26	30	50	24	57	32
7	9.03	2.93	32%	49	40	0	0	0	40
8	11.19	10.54	94%	51	72	0	0	0	0
Mean	11.19	6.02	54%	42	54	28	15	45	26
						Total	35 ^d	Total	35 ^d
SD	2.48	4.16	29%	31	64	30	21	49	23
						Total	43 ^d	Total	40 ^d

Notes: ^a graft length is the sum of the superior and inferior luminal length; ^b NIH 1/2/3/4 anastomosis: NIH measured in four different regions near the proximal and distal anastomosis; ^c NIH 5/6 mid graft: NIH measured in two different regions of the mid graft; ^d significance of difference: $p = 0.978$; NIH: neointima hyperplasia; SD: standard deviation.

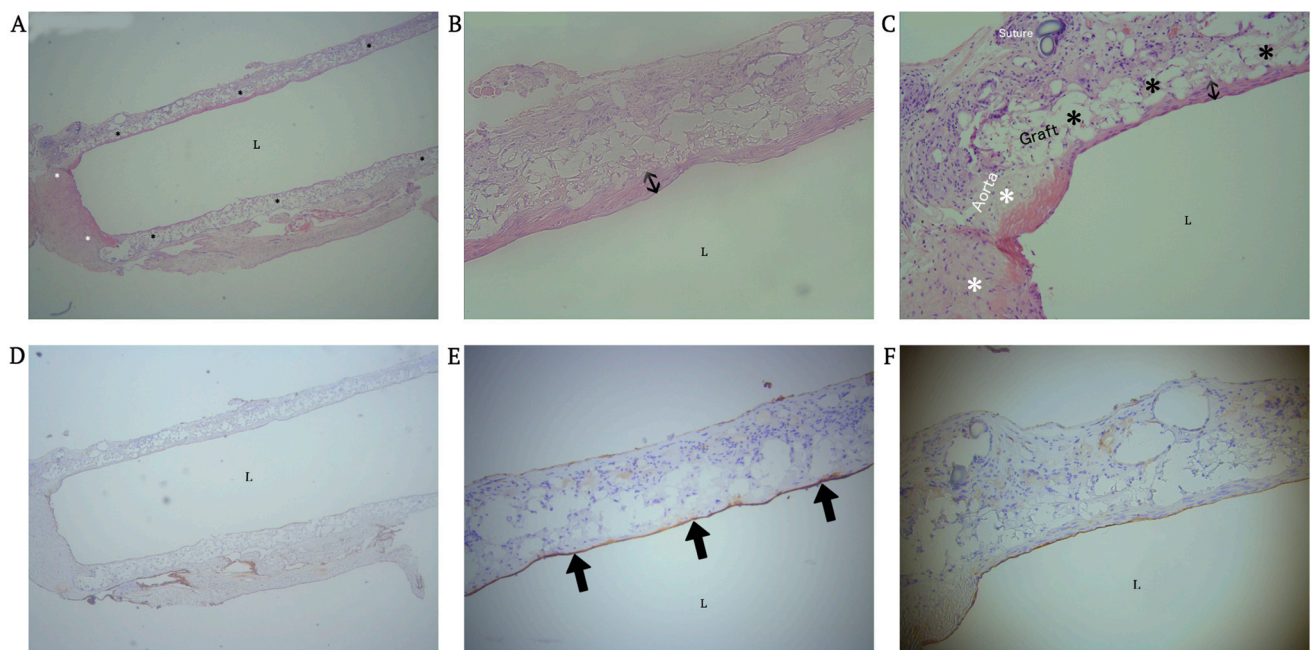


Figure 6. Upper row: neointimal hyperplasia of the graft via H&E staining. (A) (4 \times): the overview shows various neointimal thicknesses along the six regions of the graft (asterisk). No stenotic processes were observed; L = luminal side. (B) (20 \times): the mid-portion of the graft shows various thin cell layers of NIH (double-sided arrow). (C) (20 \times): anastomosis site; confluent transition between aorta (white asterisk) and the ePU graft (black asterisk). Lower row: neo-endothelialization of the graft via Anti-FVIII immunohistochemistry. (D) (4 \times): the overview shows complete endothelialization of the graft. (E) (20 \times): the mid-portion of the graft shows confluent endothelialization (black arrows) and ingrowth of cells in the porous cavities (blue-stained cells). The staining on the outer side of the graft is an artifact due to fibrous staining. (F) (20 \times): anastomosis site; transition between aorta and graft.

NE in the intervention group was measured on the anti-FVIII stained sections of the ePU grafts. NE over the course of the luminal graft length was $80 \pm 40\%$. The mean NE length was 8.95 ± 4.64 mm, covering a mean graft length of 11.19 ± 2.48 mm. One out of eight grafts did not exhibit NE. The proximal, mid-portion, and distal regions of the graft

lumen were nearly confluent positive for anti-FVIII staining. These data are summarized in Table 3. An example of NE is shown in Figure 6.

Table 3. NE on anti-FVIII immunohistochemistry of the intervention group. NE was $80 \pm 40\%$ over the course of the graft length. A total of 1/8 of the grafts showed no NE.

Subject	Graft Length (mm)	Endothelial Length (mm)	Endothelial Length/Graft Length (%)
1	9.20	5	55%
2	10.63	11	100%
3	14.38	0	0%
4	9.88	10	100%
5	16.09	17	90%
6	9.15	9	100%
7	9.03	9	100%
8	11.19	11	94%
Mean	11.19	8.95	80%
SD	2.48	4.64	40%

Notes: NE: neo-endothelialization; SD: standard deviation.

4. Discussion

The current standard for small caliber (<6 mm ID) vascular grafting in cerebral revascularization surgery is the interposition of an autologous graft, such as the GSV or the RA [2,4]. Despite the histological tissue supremacy of these autologous substitutes, technical issues and surgical complications necessitate the development of a synthetic alternative [5–7].

Yet, due to NIH and thrombosis, the use of synthetic vascular grafts using classical biomaterials such as PTFE and PET has mainly been restricted to large caliber vascular surgery [9,10,12–14]. In cardiovascular research, electrospinning is a promising technique for the development of small caliber (<6 mm ID) vascular grafts. Several reports have suggested superior in vitro and in vivo animal performance of ePU when compared to that of other organic polymers in terms of patency, absence of thrombosis, NIH, and NE [23–27]. To date, no studies have been performed evaluating the in vivo use of ePU grafts with an ID < 1.5 mm. Considering the introduction of synthetic grafts in cerebral revascularization surgery, we developed a novel ePU graft with an ID of 1.25 mm. Detailed feature characterization was performed using SEM. The ePU graft was implanted in the infrarenal aorta of rats and evaluated for patency, thrombosis, NIH, and NE after a 4-month period. The results were compared to those of the control group who underwent sham surgery. We first hypothesized that the intervention group would exhibit non-inferiority towards the control group regarding aortic patency and thrombosis. Secondly, we expected minimal differences in hemodynamic performance via ultrasound. Thirdly, upon histological examination, we expected minimal NIH and confluent NE throughout the regions of the ePU graft.

By means of SEM imaging after electrospinning, an ePU graft with small fibers of $2.0 \pm 1.43 \mu\text{m}$ was observed. The pore diameter was $5.65 \pm 2.30 \mu\text{m}$, large enough for cellular infiltration, as demonstrated by the ingrowth of different cells upon tissue slide examination. The wall thickness was $223 \pm 18 \mu\text{m}$, which was similar to the wall thickness of the GSV (250–370 μm), the current standard for small caliber vascular replacement surgery [28,29].

Some grafts showed an irregular topography, with beads in the fibers. These distortions suggest the presence of electrospinning during the electrospinning process, which is the breakup of low-viscosity solutions into droplets due to surface tension effects. This can be corrected by lowering the concentration of the polyurethane solution or by altering the solvent [30]. Our study was an initial pilot study to assess the efficacy of our novel ePU graft. In the future, larger animal studies will be required to fine-tune more of the appropriate settings of the electrospinning process (e.g., flow rate, rotation speed, needle diameter, voltage) and to investigate their potential clinical repercussions. Furthermore, the fiber diameter was variable ($2.02 \pm 1.43 \mu\text{m}$). This could be caused by temporary decreases in voltage, the interruption of the electrospinning process, or by the previously mentioned

electrospraying [30,31]. A regular fiber diameter of $<1 \mu\text{m}$ may have been preferable, as an in vitro study by Milleret et al. demonstrated less coagulation and platelet adherence with fibers $<1 \mu\text{m}$ compared to that noted using a 2–3 μm size; however, they used in vitro ePU disks instead of in vivo tubular grafts [32]. The irregular fiber orientation can also be ameliorated by adjusting the rotation speed of the mandrel [24].

The implantation of the ePU grafts was successful, as demonstrated by a favorable postoperative outcome in 8 out of 9 rats after a 4-month period. One rat was euthanized on the first postoperative day due to suspicion of graft thrombosis, which was later confirmed by histological examination. To determine the cause of the thrombotic event, the postoperative reports were examined, and these showed that temporary ligation of an undefined aortic branch (either iliolumbar or genital) close to the anastomosis region, as well as the consequent excess manipulation of the endothelium, may have led to thrombosis. Secondly, a hemostatic patch (Surgicel[®], Ethicon, Johnson&Johnson, Sommerville, NJ, USA) was used to reduce anastomosis bleeding after clamp release. The thrombogenic hemostatic fibers may have entered the graft lumen. A third possible explanation is the early graft failure on the first postoperative day, elicited by foreign body thrombosis. However, this was unlikely, as no inflammatory infiltrates were observed during histological analyses. Furthermore, immunogenic reactions are not frequently found with ePU (see introduction). Fourth, thrombosis due to NIH or insufficient NE is also unlikely because NIH in synthetic grafts only develops after two weeks and typically peaks after one month [33]. Consequently, it was too soon to observe NIH or NE during histological analyses.

Apart from this single observed case of thrombosis, neither group demonstrated clinical signs of graft/control aortic thrombosis, bringing the overall thrombosis rate of the intervention group to 1/9 (11%) compared to 0/9 (0%) in the control group, which is not significantly different. Thus, we conclude (taking the small sample size of our pilot study into account, along with a single case of thrombosis due to technical reasons) that the incidence of thrombosis in the 1.25 mm ePU graft was comparable to the incidence of thrombosis in the native aorta after sham surgery.

During ultrasound imaging, using pulsatile arterial flow in the distal aortic segment as a criterion, there was a good patency of the ePU grafts after a period of 4 months. Taking into account the aforementioned single case of thrombosis and its presumed technical cause, the intervention group held a patency of 8/9 (89%) compared to 9/9 (100%) in the control group, which was not clinically significantly different. Therefore, the patency of the ePU grafts was comparable to the patency of the native aorta after sham surgery. A recent study by Bergmeister et al. reported patency rates of 95% 6 months after implantation of 1.50 mm ID ePU grafts into the infrarenal aorta of rats [34]. A shortcoming in this study was the lack of a control group; however, the patency rates were good and were comparable to those obtained in our study (89% vs. 95%). There are no other published in vivo studies utilizing chemically unblended ePU grafts with smaller diameters ($<1.25 \text{ mm ID}$). Nieponice et al. investigated the in vivo performance of 1.20 mm ID ePU grafts seeded with muscle-derived stem cells in the infrarenal aortas of rats, with patency rates of 65% after 2 months, which was lower than the 89% observed in our study [35].

Via ultrasound, there was a statistically significant ($p = 0.010$) difference in V_{max} decay throughout the graft between the intervention group and the control group. The difference in distal aortic systolic expansion was present but was not statistically significant ($p = 0.353$) between groups; however, the small sample size of our pilot study may have been a source of underestimation of the effect. The loss of velocity and the limited loss of aortic systolic expansion over the course of the ePU graft suggest a loss of energy of the blood because of a higher resistance of the graft compared to that of the native aorta. A first potential cause of energy loss is graft stenosis, although this was unlikely because a stenotic segment would exhibit an increased flow velocity. The mean V_{max} in the mid-graft was lower than at the proximal and distal end of the graft. Leakage of the graft may have been a second potential cause; however, in vivo evaluation during retrieval revealed a watertight anastomosis. Third, and more likely, is a lower elasticity of the graft compared to that of the

native aorta, inducing an increase in resistance and loss of kinetic energy. The differences in absolute Vmax throughout the graft were not significant between the intervention and control group and neither were the proximal and distal systolic expansion rates.

Regardless of the fact that there was only one statistically significant hemodynamic difference between the groups (Vmax decay), the abovementioned findings suggest a slight mechanical incompatibility of the ePU graft *in vivo*. This may be a possible factor to take into account for future optimizations of the hemodynamic capacities of the graft.

H&E histological analyses after the 4-month study period did not demonstrate any significant or stenotic NIH in the ePU grafts ($35 \pm 42 \mu\text{m}$, $54 \pm 29\%$ of the graft length); compared to those noted in other studies in the literature, and in 1/8 grafts, no NIH was apparent. NIH is a consequence of shear stress caused by turbulent blood flow and, as mentioned previously, it normally only reaches its maximum after 1 month [36]. Thus, because there was only minimal NIH after a 4-month period, it was unlikely that there would be any further increases over a longer period of time. Interestingly, in a recent report from Bergmeister et al., it was demonstrated that there were only 2/20 ePU grafts with visible NIH after 3 months (mid graft: mean $198 \pm 73 \mu\text{m}$, anastomoses: mean $159 \pm 71 \mu\text{m}$). There are two potential reasons for the smaller NIH rates found in the Bergmeister et al. study compared to those observed in our study: (1) size-mismatch; the ID of the infrarenal aorta of the rat ranged from 1 to 2 mm [19]. Size-mismatch in our study may have led to shear stress conditions and subsequent NIH. However, as is evident from Figure 4, there was no size mismatch in our study [37]. (2) NIH may have been caused by incomplete endothelialization, which is more likely, as described below [34].

Immunohistochemistry staining with anti-FVIII for NE demonstrated $80 \pm 40\%$ luminal coverage of the ePU graft length (mean NE length $8.95 \pm 4.64 \text{ mm}$, covering a mean graft length of $11.19 \pm 2.48 \text{ mm}$). This was probably an underestimation due to cutting artefacts with the microtome. The endothelial coverage is an indicator that the porous structure of the ePU graft facilitates the migration and engraftment of endothelial cells, protecting the graft from shear stress and thrombosis. Given the very low incidence of thrombotic events in our study, NE was likely sufficiently protective. The promotion of NE in ePU grafts has been demonstrated in previous studies by Uttayarat et al. (ID 2.10 mm), Grasl and Bergmeister et al. (ID 1.74/2.10 mm), and in other studies that used larger IDs [18,23,38,39]. NE was demonstrated *in vivo* after a 1-month study period by Bergmeister et al. (ID 1.50 mm, infrarenal aorta of rats) [34]. The added value of our study is the clear evidence of similar NE in ePU grafts with ID 1.25 mm.

The ID of our graft (1.25 mm) is smaller than the ID of grafts used in previous studies to investigate the *in vivo* performance of ePU grafts (Bergmeister and Grasl studies, ID $\geq 1.50 \text{ mm}$). Some groups have performed *in vivo* testing using smaller IDs (starting from 0.70 mm); however, they used more complex electrospun materials with the addition of multiple chemical chains [12,40]. For instance, some groups used poly(ϵ -caprolactone) with the addition of chitosan (ID 1 mm, Fukunishi et al.) [41], poly(glycerol sebacate) (ID 0.72 mm, Wu et al.) [42], poly(L-lactic acid) (ID 1 mm, He et al.) [43], and cysteine-alanine-glycine (ID 0.7 mm, Kuwabara et al.) [44]. Other groups used amino acid-based poly(ester urea) (ID 1 mm, Gao et al.) [45], plasma-heparin-treated polycarbonate urethane (ID 1 mm, Qiu et al.) [46], polyethylene glycol and mucin (ID 1 mm, Janairo et al.) [47], or polyethylene glycol, polylactic acid, and hirudin (ID 1 mm, Hashi et al.) [48]. Additionally, some groups have investigated the seeding of small electrospun grafts with various cells, for instance poly(ester urethane) urea seeded with muscle stem cells (ID 1.2 mm, Nieponice et al.) [35] or poly(L-lactic acid) seeded with mesenchymal stem cells (ID 0.7 mm, Hashi et al.) [49]. These studies were all single studies with limited sample sizes (3 to 46 animals) or with a lack of adequate control groups and variable patency rates. However, some of these studies reported reasonable patency results compared to those in our study (89%): Qiu et al. (common carotid artery (CCA) rats, $n = 14$, 86% patency) [46], Kuwabara et al. (CCA rats, $n = 46$, 77% patency) [44], Janairo et al. (CCA rats, $n = 8$, 100% patency) [47], Sun et al. (spider silk protein grafts with ID 1.2 mm in

abdominal aorta rats, $n = 15$, 75–85% patency) [50], and Wakabayashi et al. (polyvinyl alcohol coated polycaprolactone grafts with ID 1 mm, $n = 12$, 83.3% patency) [51]. Therefore, other biomaterials may also be promising candidates, along with ePU. Also, preclinical studies have been performed with acellular extracellular matrices from animals [52].

There are some potential limitations to our study. Firstly, there was a small sample size ($n = 18$), with possible over- or underestimation of the results. Secondly, the graft had a short length (7.5 mm). In future studies, it would be interesting to investigate the ePU graft on longer trajectories because lengths starting from 2 cm provide more challenges for endothelialization. The infrarenal aorta of the Wistar rat is not long enough, so a femoral artery crossover graft could be used instead, or alternatively, larger animals, such as rabbits, sheep, or pigs, which exhibit less spontaneous endothelialization and have a greater tendency for hypercoagulability, could also be used [19].

Despite the good hemodynamic resemblance between rat aortas and cerebral blood vessels, the extrapolation of our results to humans should be performed with caution. Rats have a stronger fibrinolytic system and increased spontaneous endothelialization; subsequently, there is a potential underestimation of thrombosis incidence [19]. To date, no clinical studies have been performed using ePU grafts, and studies with larger sample sizes in different (larger) animal models are needed to further confirm the good in vivo performance of ePU grafts with ID < 1.50 mm. Animal studies thus far have failed to translate into clinical trials due to insufficient in vivo mechanical testing and regulatory issues [19,50].

The ePU graft possesses several good characteristics of an arterial prosthesis (as described by Abbott et al.) [53]. We, along with others, would like to reiterate the necessity for more and larger long-term studies on various animal models to determine the efficacy of small caliber ePU grafts [18]. This could lead to the development of more clinically efficacious graft substitutes for use in small caliber vascular surgery, such as cerebral revascularization.

5. Conclusions

Our results clearly demonstrate that ePU grafts are potentially efficacious synthetic alternatives for autologous vascular grafts. We have shown that, after fine-tuning the electrospinning process, ePU vascular grafts are also potentially good substitutes for use in small caliber vascular surgery with IDs < 1.50 mm, e.g., cerebral revascularization.

The graft can be sterilized, is not expensive, is easy to suture, can be easily produce in various IDs, and shows durability.

Author Contributions: E.V., M.R.L.T. and T.M. were the major contributors in regards to conducting the experiments and writing the manuscript. A.H. and S.V.V. contributed to the technical development of the electrospun graft. M.D. and G.R.Y.D.M. aided with ultrasound imaging, and P.P. provided insights into the histological evaluations. All authors have read and agreed to the published version of the manuscript.

Funding: This work was supported with equipment (high frequency ultrasound, VEVO[®] 2100, Visualsonics Inc.) funded by a Hercules grant from the Flemish Research Fund (AUHA/13/03).

Institutional Review Board Statement: This study was approved by the Ethical Committee for Animal Experiments at the University of Antwerp (approval number 2015-55).

Informed Consent Statement: Not applicable.

Data Availability Statement: The data presented in this study are available on request from the corresponding author. The data are not publicly available due to technical reasons, as some of the data is written on paper and some of the data is included in the used software.

Acknowledgments: We are grateful to Bronwen Martin for her thorough reviewing and English editing of our paper. We also acknowledge Krystyna Szewczyk, Annemie Van Eetveldt, the caregivers of the animalarium and veterinary practice “De Vroente”, for their knowledge of animal surgery. We thank Siegrid Pauwels and Rita Van Den Bossche for their help with the histology, as well as the rats for their sacrifices, for which we are ever grateful.

Conflicts of Interest: The authors declare no conflict of interest.

Abbreviations

ePU	electrospun polyurethane
GSV	great saphenous vein
ID	inner diameter
IDps, IDpd, IDds, IDdd,	inner/outer, proximal/distal diameters
ODps, ODpd, ODds and ODpd	and systolic/diastolic diameters of graft/control aortas
NE	neo-endothelialization
NIH	neointimal hyperplasia
RA	radial artery
SEM	scanning electron microscopy

References

- Charbel, F.; Amin-Hanjani, S. Decision making in cerebral revascularization surgery using intraoperative CBF measurements. In *Cerebral Revascularization*, 1st ed.; Elsevier/Saunders: Philadelphia, PA, USA, 2011; p. 44.
- Liu, J.K.; Kan, P.; Karwande, S.V.; Couldwell, W.T. Conduits for cerebrovascular bypass and lessons learned from the cardiovascular experience. *Neurosurg. Focus* **2003**, *14*, e3. [[CrossRef](#)] [[PubMed](#)]
- Archie, J.P. Carotid endarterectomy saphenous vein patch rupture revisited: Selective use on the basis of vein diameter. *J. Vasc. Surg.* **1996**, *24*, 346–351. [[CrossRef](#)] [[PubMed](#)]
- Greenberg, M.; Abel, N. Stroke and occlusive cerebrovascular disease. In *Greenberg Handbook of Neurosurgery*, 8th ed.; Thieme: New York, NY, USA, 2016; p. 1318.
- Eddleman, C.; Getch, C.; Bendok, B.; Batjer, H. Saphenous vein grafts for the high-flow cerebral revascularization. In *Cerebral Revascularization*, 1st ed.; Elsevier/Saunders: Philadelphia, PA, USA, 2011; pp. 125–126.
- Surdell, D.L.; Hage, Z.A.; Eddleman, C.S.; Gupta, D.K.; Bendok, B.R.; Batjer, H.H. Revascularization for complex intracranial aneurysms. *Neurosurg. Focus* **2008**, *24*, E21. [[CrossRef](#)] [[PubMed](#)]
- Sweeney, J.; Sasaki-Adams, D.; Abdulrauf, S. Radial artery harvesting for cerebral revascularization: Technical pearls. In *Cerebral Revascularization*, 1st ed.; Elsevier/Saunders: Philadelphia, PA, USA, 2011; pp. 119–120.
- Kawashima, M.; Rhoton, A., Jr. Surgical anatomy of EC-IC bypass procedures. In *Cerebral Revascularization*, 1st ed.; Elsevier/Saunders: Philadelphia, PA, USA, 2011; p. 66.
- Stegemann, J.P.; Kaszuba, S.N.; Rowe, S.L. Review: Advances in vascular tissue engineering using protein-based biomaterials. *Tissue Eng.* **2007**, *13*, 2601–2613. [[CrossRef](#)] [[PubMed](#)]
- Sankaran, K.K.; Subramanian, A.; Krishnan, U.M.; Sethuraman, S. Nanoarchitecture of scaffolds and endothelial cells in engineering small diameter vascular grafts. *Biotechnol. J.* **2015**, *10*, 96–108. [[CrossRef](#)]
- Sayers, R.D.; Raptis, S.; Berce, M.; Miller, J.H. Long-term results of femorotibial bypass with vein or polytetrafluoroethylene. *Br. J. Surg.* **1998**, *85*, 934–938. [[CrossRef](#)]
- Kucinska-Lipka, J.; Gubanska, I.; Janik, H.; Sienkiewicz, M. Fabrication of polyurethane and polyurethane based composite fibres by the electrospinning technique for soft tissue engineering of cardiovascular system. *Mater. Sci. Eng. C Mater. Biol. Appl.* **2015**, *46*, 166–176. [[CrossRef](#)]
- Xue, L.; Greisler, H.P. Biomaterials in the development and future of vascular grafts. *J. Vasc. Surg.* **2003**, *37*, 472–480. [[CrossRef](#)]
- Abbott, W.M.; Vignati, J.J. Prosthetic grafts: When are they a reasonable alternative? *Semin. Vasc. Surg.* **1995**, *8*, 236–245.
- Li, D.; Xia, Y. Electrospinning of Nanofibers: Reinventing the Wheel? *Adv. Mater.* **2004**, *16*, 1151–1170. [[CrossRef](#)]
- Sill, T.J.; von Recum, H.A. Electrospinning: Applications in drug delivery and tissue engineering. *Biomaterials* **2008**, *29*, 1989–2006. [[CrossRef](#)] [[PubMed](#)]
- Uthamaraj, S.; Tefft, B.J.; Jana, S.; Hlinomaz, O.; Kalra, M.; Lerman, A.; Dragomir-Daescu, D.; Sandhu, G.S. Fabrication of Small Caliber Stent-grafts Using Electrospinning and Balloon Expandable Bare Metal Stents. *J. Vis. Exp.* **2016**, *116*, e54731. [[CrossRef](#)]
- Ercolani, E.; Del, G.C.; Bianco, A. Vascular tissue engineering of small-diameter blood vessels: Reviewing the electrospinning approach. *J. Tissue Eng. Regen. Med.* **2015**, *9*, 861–888. [[CrossRef](#)]
- Byrom, M.J.; Bannon, P.G.; White, G.H.; Ng, M.K. Animal models for the assessment of novel vascular conduits. *J. Vasc. Surg.* **2010**, *52*, 176–195. [[CrossRef](#)] [[PubMed](#)]
- Council, N.R. *Guide for the Care and Use of Laboratory Animals*, 8th ed.; The National Academic Press: Washington DC, USA, 2011.
- Kilkenny, C.; Browne, W.J.; Cuthill, I.C.; Emerson, M.; Altman, D.G. Improving bioscience research reporting: The ARRIVE guidelines for reporting animal research. *PLoS Biol.* **2010**, *8*, e1000412. [[CrossRef](#)]
- Morton, D.; Hau, J. Welfare assesment and humane endpoints. In *Handbook of Laboratory Animal Science*, 2nd ed.; CRC Press: Boca Raton, FL, USA, 2003; Volume 1, pp. 468–472.
- Grasl, C.; Bergmeister, H.; Stoiber, M.; Schima, H.; Weigel, G. Electrospun polyurethane vascular grafts: In vitro mechanical behavior and endothelial adhesion molecule expression. *J. Biomed. Mater. Res. A* **2010**, *93*, 716–723. [[CrossRef](#)]

24. He, W.; Hu, Z.; Xu, A.; Liu, R.; Yin, H.; Wang, J.; Wang, S. The preparation and performance of a new polyurethane vascular prosthesis. *Cell Biochem. Biophys.* **2013**, *66*, 855–866. [[CrossRef](#)]
25. He, W.; Hu, Z.J.; Xu, A.W.; Yin, H.H.; Wang, J.S.; Ye, J.L.; Wang, S.M. Assessment of the mechanical properties and biocompatibility of a new electrospun polyurethane vascular prosthesis. *Nan Fang Yi Ke Da Xue Xue Bao* **2011**, *31*, 2006–2011.
26. Wang, X.; Lin, P.; Yao, Q.; Chen, C. Development of small-diameter vascular grafts. *World J. Surg.* **2007**, *31*, 682–689. [[CrossRef](#)]
27. Sell, S.A.; McClure, M.J.; Garg, K.; Wolfe, P.S.; Bowlin, G.L. Electrospinning of collagen/biopolymers for regenerative medicine and cardiovascular tissue engineering. *Adv. Drug Deliv. Rev.* **2009**, *61*, 1007–1019. [[CrossRef](#)] [[PubMed](#)]
28. Konig, G.; McAllister, T.N.; Dusserre, N.; Garrido, S.A.; Iyican, C.; Marini, A.; Fiorillo, A.; Avila, H.; Wystrychowski, W.; Zagalski, K.; et al. Mechanical properties of completely autologous human tissue engineered blood vessels compared to human saphenous vein and mammary artery. *Biomaterials* **2009**, *30*, 1542–1550. [[CrossRef](#)] [[PubMed](#)]
29. Donovan, D.L.; Schmidt, S.P.; Townshend, S.P.; Njus, G.O.; Sharp, W.V. Material and structural characterization of human saphenous vein. *J. Vasc. Surg.* **1990**, *12*, 531–537. [[CrossRef](#)] [[PubMed](#)]
30. Pillay, V.; Dott, C.; Choonara, Y.E.; Tyagi, C.; Tomar, L.; Kumar, P.; Toit, L.C.D.; Ndesendo, V.M.K. A Review of the Effect of Processing Variables on the Fabrication of Electrospun Nanofibers for Drug Delivery Applications. *J. Nanomater.* **2017**, *2013*, 789289. [[CrossRef](#)]
31. Beachley, V.; Wen, X. Effect of electrospinning parameters on the nanofiber diameter and length. *Mater. Sci. Eng. C Mater. Biol. Appl.* **2009**, *29*, 663–668. [[CrossRef](#)] [[PubMed](#)]
32. Milleret, V.; Hefti, T.; Hall, H.; Vogel, V.; Eberli, D. Influence of the fiber diameter and surface roughness of electrospun vascular grafts on blood activation. *Acta Biomater.* **2012**, *8*, 4349–4356. [[CrossRef](#)] [[PubMed](#)]
33. Beattie, D.; Davies, A. Graft maintenance and graft failure. In *Emergency Vascular and Endovascular Surgical Practice*, 2nd ed.; Barros, A., Chant, A., Eds.; Hodder Arnold: London, UK, 2017; pp. 197–199.
34. Bergmeister, H.; Grasl, C.; Walter, I.; Plasenzotti, R.; Stoiber, M.; Schreiber, C.; Losert, U.; Weigel, G.; Schima, H. Electrospun small-diameter polyurethane vascular grafts: Ingrowth and differentiation of vascular-specific host cells. *Artif. Organs* **2012**, *36*, 54–61. [[CrossRef](#)] [[PubMed](#)]
35. Nieponice, A.; Soletti, L.; Guan, J.; Hong, Y.; Gharaibeh, B.; Maul, T.M.; Huard, J.; Wagner, W.R.; Vorp, D.A. In vivo assessment of a tissue-engineered vascular graft combining a biodegradable elastomeric scaffold and muscle-derived stem cells in a rat model. *Tissue Eng. Part A* **2010**, *16*, 1215–1223. [[CrossRef](#)]
36. Waltham, M.; Harris, J. Intimal hyperplasia: The nemesis of cardiovascular intervention. *ANZ J. Surg.* **2004**, *74*, 719–720. [[CrossRef](#)]
37. Zilla, P.; Bezuidenhout, D.; Human, P. Prosthetic vascular grafts: Wrong models, wrong questions and no healing. *Biomaterials* **2007**, *28*, 5009–5027. [[CrossRef](#)]
38. Uttayarat, P.; Perets, A.; Li, M.; Pimton, P.; Stachelek, S.J.; Alferiev, I.; Composto, R.J.; Levy, R.J.; Lelkes, P.I. Micropatterning of three-dimensional electrospun polyurethane vascular grafts. *Acta Biomater.* **2010**, *6*, 4229–4237. [[CrossRef](#)]
39. Bergmeister, H.; Schreiber, C.; Grasl, C.; Walter, I.; Plasenzotti, R.; Stoiber, M.; Bernhard, D.; Schima, H. Healing characteristics of electrospun polyurethane grafts with various porosities. *Acta Biomater.* **2013**, *9*, 6032–6040. [[CrossRef](#)] [[PubMed](#)]
40. Rocco, K.A.; Maxfield, M.W.; Best, C.A.; Dean, E.W.; Breuer, C.K. In vivo applications of electrospun tissue-engineered vascular grafts: A review. *Tissue Eng. Part B Rev.* **2014**, *20*, 628–640. [[CrossRef](#)] [[PubMed](#)]
41. Fukunishi, T.; Best, C.A.; Sugiura, T.; Shoji, T.; Yi, T.; Udelsman, B.; Ohst, D.; Ong, C.S.; Zhang, H.; Shinoka, T.; et al. Tissue-Engineered Small Diameter Arterial Vascular Grafts from Cell-Free Nanofiber PCL/Chitosan Scaffolds in a Sheep Model. *PLoS ONE* **2016**, *11*, e0158555. [[CrossRef](#)] [[PubMed](#)]
42. Wu, W.; Allen, R.A.; Wang, Y. Fast-degrading elastomer enables rapid remodeling of a cell-free synthetic graft into a neoartery. *Nat. Med.* **2012**, *18*, 1148–1153. [[CrossRef](#)] [[PubMed](#)]
43. He, W.; Ma, Z.; Teo, W.E.; Dong, Y.X.; Robless, P.A.; Lim, T.C.; Ramakrishna, S. Tubular nanofiber scaffolds for tissue engineered small-diameter vascular grafts. *J. Biomed. Mater. Res. A* **2009**, *90*, 205–216. [[CrossRef](#)] [[PubMed](#)]
44. Kuwabara, F.; Narita, Y.; Yamawaki-Ogata, A.; Kanie, K.; Kato, R.; Satake, M.; Kaneko, H.; Oshima, H.; Usui, A.; Ueda, Y. Novel small-caliber vascular grafts with trimeric Peptide for acceleration of endothelialization. *Ann. Thorac. Surg.* **2012**, *93*, 156–163. [[CrossRef](#)] [[PubMed](#)]
45. Gao, Y.; Yi, T.; Shinoka, T.; Lee, Y.U.; Reneker, D.H.; Breuer, C.K.; Becker, M.L. Pilot Mouse Study of 1 mm Inner Diameter (ID) Vascular Graft Using Electrospun Poly(ester urea) Nanofibers. *Adv. Healthc. Mater.* **2016**, *5*, 2427–2436. [[CrossRef](#)]
46. Qiu, X.; Lee, B.L.; Ning, X.; Murthy, N.; Dong, N.; Li, S. End-point immobilization of heparin on plasma-treated surface of electrospun polycarbonate-urethane vascular graft. *Acta Biomater.* **2017**, *51*, 138–147. [[CrossRef](#)]
47. Janairo, R.R.; Zhu, Y.; Chen, T.; Li, S. Mucin covalently bonded to microfibers improves the patency of vascular grafts. *Tissue Eng. Part A* **2014**, *20*, 285–293. [[CrossRef](#)]
48. Hashi, C.K.; Derugin, N.; Janairo, R.R.; Lee, R.; Schultz, D.; Lotz, J.; Li, S. Antithrombogenic modification of small-diameter microfibrillar vascular grafts. *Arterioscler. Thromb. Vasc. Biol.* **2010**, *30*, 1621–1627. [[CrossRef](#)]
49. Hashi, C.K.; Zhu, Y.; Yang, G.Y.; Young, W.L.; Hsiao, B.S.; Wang, K.; Chu, B.; Li, S. Antithrombogenic property of bone marrow mesenchymal stem cells in nanofibrillar vascular grafts. *Proc. Natl. Acad. Sci. USA* **2007**, *104*, 11915–11920. [[CrossRef](#)] [[PubMed](#)]

50. Sun, L.; Li, X.; Yang, T.; Lu, T.; Du, P.; Jing, C.; Chen, Z.; Lin, F.; Zhao, G.; Zhao, L. Construction of spider silk protein small-caliber tissue engineering vascular grafts based on dynamic culture and its performance evaluation. *J. Biomed. Mater. Res. A* **2023**, *111*, 71–87. [[CrossRef](#)] [[PubMed](#)]
51. Wakabayashi, N.; Yoshida, T.; Oyama, K.; Naruse, D.; Tsutsui, M.; Kikuchi, Y.; Koga, D.; Kamiya, H. Polyvinyl alcohol coating prevents platelet adsorption and improves mechanical property of polycaprolactone-based small-caliber vascular graft. *Front. Cardiovasc. Med.* **2022**, *9*, 946899. [[CrossRef](#)] [[PubMed](#)]
52. Ilanlou, S.; Khakbiz, M.; Amoabediny, G.; Mohammadi, J. Preclinical studies of acellular extracellular matrices as small-caliber vascular grafts. *Tissue Cell* **2019**, *60*, 25–32. [[CrossRef](#)]
53. Abbott, W.M.; Callow, A.; Moore, W.; Rutherford, R.; Veith, F.; Weinberg, S. Evaluation and performance standards for arterial prostheses. *J. Vasc. Surg.* **1993**, *17*, 746–756. [[CrossRef](#)]

Disclaimer/Publisher’s Note: The statements, opinions and data contained in all publications are solely those of the individual author(s) and contributor(s) and not of MDPI and/or the editor(s). MDPI and/or the editor(s) disclaim responsibility for any injury to people or property resulting from any ideas, methods, instructions or products referred to in the content.